

# RCS Modelling of Extended Targets Using Supervised Learning

F. Ahmad<sup>1</sup>, M.M.H. Amir<sup>1</sup>, S. Maresca<sup>2</sup>, A. Malacarne<sup>3</sup>, A. Bogoni<sup>1,3</sup> and M. Scaffardi<sup>3</sup>

<sup>1</sup>Sant'Anna School of Advanced Studies, TeCIP Institute, 56124, Pisa, Italy

<sup>2</sup>CNR-IEIIT 56124, Pisa, Italy

<sup>3</sup>CNIT - Photonic Networks & Technologies National Laboratory (PNTLab), 56124, Pisa, Italy

**Abstract**—Knowing the Radar Cross Section (RCS) of specific targets is of primary importance in target detection and recognition. The RCS may significantly vary with radar operating frequency and target's size, shape, material, and orientation with respect to radar illumination direction. Thus, a time-efficient way to model target RCS is of paramount importance in simulating close-to-reality scenarios where the position and orientation of target frequently vary. In this paper, an efficient estimation technique using machine learning algorithm is presented that can predict the RCS of targets of any shape and size. The proposed method is compared with the RCS obtained from the MATLAB tool POfacets. Computational time and mean square error (MSE) of estimated RCS with respect to the actual one are used as performance metrics.

**Keywords**—Machine learning (ML), MIMO Radars, Physical Optics (PO), Radar Cross Section (RCS) Modeling.

## I. INTRODUCTION

In recent decades, radar technology has undergone continuous developments both in system architecture and processing domain. To overcome the constraints of monostatic systems, the research has been focused on multiple-input multiple-output (MIMO) systems, capable of exploiting spatial diversity for a finer resolution and better sensitivity [1], [2].

MIMO radars can be distinguished in two main types: (i) MIMO radar with co-located antennas [3] and (ii) MIMO radars with widely separated antennas [4]. The former exploits waveform diversity (WD) and demonstrates superiority over phased array radar for parameter estimation and flexibility in designing beampatterns, while the latter tackles the problem of RCS fluctuation and detection of slow-moving targets by exploiting the geometric diversity (GD) [5].

Among the numerous challenges encountered while implementing distributed MIMO radar systems, radar cross section (RCS) estimation remains a highly debated and extensively researched functionality [6]. RCS is the electromagnetic area of the target as seen by the radar. It describes the amount of energy backscattered towards the radar receiver, and it is influenced not only by waveform characteristics (e.g., carrier frequency), target size, shape and material, but also by the target-sensor geometry. Even a small variation of the above-mentioned parameters can result in large RCS variation which in turn affects the detection capability of the radar system.

There are two methods for estimating RCS, i.e., exact, and approximate methods [7]. To overcome computational complexity, approximate methods are mostly preferred [8]. Geometrical Optics (GO) and Physical Optics (PO) are two of the most used approximate models. Although the GO model is easy to implement, it comes with limitations, as it fails to predict RCS in case of flat and cylindrical surface. PO

modelling exhibits high computational load but provides good results as close to exact models. The POfacets tool developed in MATLAB is based on PO approximation providing monostatic and bistatic RCS [9]. Different works have been conducted using POfacets for calculating RCS. The work presented in [6] calculates the bistatic RCS for extended targets using POfacets. However, in a close-to-reality scenario where the target continuously changes its orientation and position with respect to the radar heads (RHs), modelling the target RCS using POfacets is computationally expensive. To tackle this issue, another method using the empirical formula is employed to estimate bistatic RCS in [10], however at the cost of reduced accuracy.

In recent years, researchers have tilted towards machine learning (ML) algorithms in various research domains. With rapid calculation and robust nonlinear representation capabilities, ML algorithms emerge as a potential replacement of conventional computational electromagnetics methods. ML models have been applied to predict the RCS of a target considering monostatic scenario, demonstrating close accuracy to actual RCS with low computational complexity [11],[12]. However, there exists a very limited body of research pertaining to the RCS estimation considering bistatic and MIMO radar scenarios.

This paper presents a significant advancement by redirecting the focus on bistatic RCS modelling for extended targets using ML techniques. To the best of our knowledge, this is the first attempt at addressing this problem. Here, the underlying assumption is that the target lays in a single radar resolution cell (i.e., narrowband signal). In other words, although the target is composed by multiple scatterers, its RCS is compressed to a single value. The case in which the target lays in multiple resolution cells (i.e., wideband signal) is currently under analysis and will be the argument of future publications.

## II. MIMO RADAR SIGNAL MODEL

Let us consider a MIMO radar system employing  $M$  transmitter (TX) antennas denoted as  $TX_m$  and  $N$  receiver (RXs) antennas as  $RX_n$ , where  $m = 1, \dots, M$  and  $n = 1, \dots, N$ . Let us assume that TX antennas illuminate  $K$  point-like scatterers  $P_k$  where  $k = 1, \dots, K$ . All TXs are operating in X-band at frequency of 9.7GHz and let the signal transmitted by each  $TX_m$  be  $s_m$ . Signal received by each  $RX_n$  is given as [4]:

$$r_{m,n}(t) = \sum_{k=1}^K a_{m,n}^k s_m(t - \tau_{m,n}^k) e^{j\varphi_{m,n}(t)} + w_n(t) \quad (1)$$

where  $a_{m,n}^{(k)}$  and  $\tau_{m,n}^{(k)}$  represents amplitude and delay respectively which depends on the bistatic geometry among  $TX_m$ ,  $RX_n$  and  $P_k$  positions. The corresponding introduced phase shift is denoted by  $\varphi_{m,n}(t)$ . The received signal is

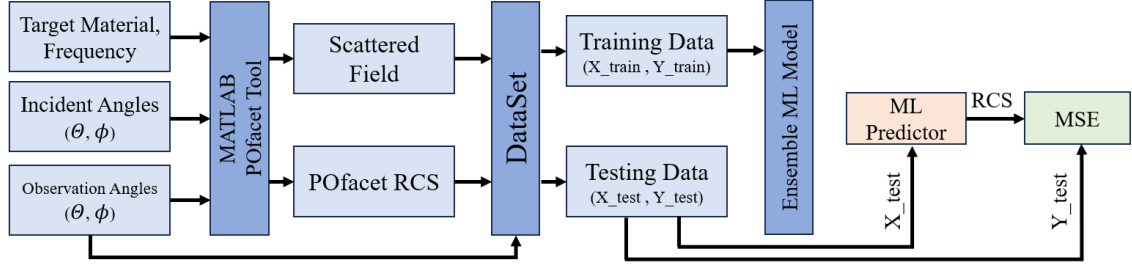


Fig. 1. Flow chart of the proposed ML-based algorithm for predicting bistatic RCS of extended targets.

affected by additive white gaussian noise (AWGN) which is denoted by  $w_n(t)$ . The generic amplitude term can be calculated as:

$$a_{m,n}^{(k)} = \sqrt{\frac{P_{TX}^m G_{TX}^m A_n \sigma_{m,n}^k}{(4\pi)^3 k_B T_n L_n d^2(TX_m, P_k) d^2(P_k, RX_m)}} \quad (2)$$

where  $P_{TX}^m$  and  $G_{TX}^m$  are the transmit power and antenna gain at  $TX_m$  respectively.  $A_n$  is the effective area of  $RX_n$ . The bistatic RCS observed by the system consisting of  $TX_m$ - $RX_n$  virtual channel is denoted by  $\sigma_{m,n}^k$  for  $P_k$  scatterer.  $k_B$  is the Boltzmann's constant,  $T_n$  and  $L_n$  are the noise temperature and loss factors at  $RX_n$  respectively. Finally,  $d^2(TX_m, P_k)$  and  $d^2(P_k, RX_m)$  are the transmitter-scatterer and scatterer-receiver Euclidean square distances.

As it is evident from Eq. (1) and Eq. (2), the received signal  $r_{m,n}(t)$  has a direct dependency on RCS  $\sigma_{m,n}^k$ , and therefore requires an accurate RCS modelling.

### III. RCS MODELLING USING MACHINE LEARNING

POfacets is one of the most common tools used for calculating RCS [9]. POfacets resolves the target model with a large number of triangular facets which are illuminated by the incident field. The scattered field components from each facet are superimposed to obtain the scattered field in the observation direction. Once the scattered field is known, the RCS in that direction is computed. The RCS of a simple point-like target in a MIMO radar scenario has been computed in [6]. However, given a close-to-reality scenario where the target orientation is continuously changing, estimating RCS using POfacets can be computationally expensive.

ML models have proven their performance in various fields exhibiting accuracy levels closely aligned with real-world scenarios at the cost of very low computational complexity. Since predicting RCS is a regression problem, there are several ML models, such as Neural Network (NN) [13], K-nearest neighbor (KNN) [14], Support Vector Machine (SVM) [15] etc., that can be implemented to predict RCS. However, to keep both accuracy and low computational complexity a priority, an ensemble ML approach is used. The ensemble approach involves training two or more models on the same dataset and the prediction of each model is combined to achieve better performance as compared to any individual model [16]. ML involves dataset generation and training which are offline processes, and testing of the model which is performed online once the model is trained. A complete block diagram is shown in Fig 1.

#### A. Dataset Generation

The proposed ML model is a supervised learning model, it is therefore important to identify inputs and outputs of the

model. Multiple input features involved in estimating RCS of a target including target shapes, position, size, material, operating frequency, azimuth and elevation of TX etc. Small variation of these parameters can lead to large RCS variation. It is reported in [1], even slight change in the look angles can cause approximately 20dB variation. It is impractical to train a ML model for all possible combinations of input features. For simplicity, among all only three features including scattered field, observe azimuth and elevation angle are considered as inputs, and the corresponding RCS as an output. Scattered field is an important feature that depends on incident angles, operating frequency and target's characteristic. It contains all the information required to estimate target's RCS. To generate the dataset the most reliable tool is POfacets which gives accurate RCS values.

A complex model of a 40-m yacht is considered from POfacets library as an extended target. Let us consider a narrow band radar illuminating the yacht such that the radar resolution cell is so large to contain the whole target. This approximates the target as a point-like scatterer and most of the RCS modeling tools rely on this assumption. To employ a bistatic scenario, the tool is provided with incidence elevation angle  $\theta_{in} = 45^\circ$ , azimuth angle  $\phi_{in} = 0^\circ$  and observation elevation angle in the range  $\theta_{ob} = 0^\circ \div 90^\circ$  with increment of  $1^\circ$  and azimuth angle in the range  $\phi_{ob} = 0^\circ \div 360^\circ$  with increment of  $1^\circ$  operating at 9.7GHz. This creates a bistatic scenario in which the incident angle is fixed while the observation angles in azimuth and elevation directions are varied along with the step of  $1^\circ$ , creating 32851 possible TX-RX combinations. Upon simulation, 32851 scattered fields are generated as input and a corresponding RCS vector of length 32851 as an output from ML. This is a complete dataset that contains X as input and Y as output combination required to train a model as shown in Fig.2.

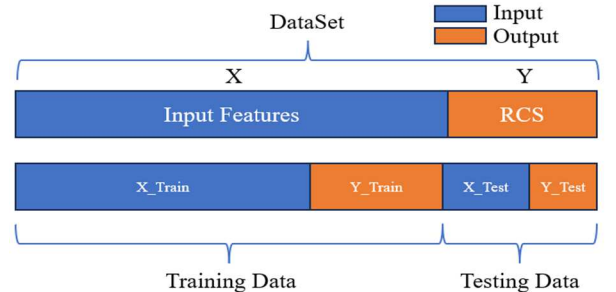


Fig. 2. Dataset for ML model

#### B. Training

Once the dataset is generated, it is split into 70% training data and 30% testing data. Testing data is kept unseen to the model during training and will be used for testing. To train a

model, training data that contain  $X_{train}$  and  $Y_{Train}$  is given to Model 1 in Fig.3. As mentioned above, the ensemble model involves the combination of multiple weak models known as base models. In this case, the base model is a decision tree with a maximum number of splits in each node set to 50. The algorithm used for ensemble learning is LSBoost [17]. There are a total of 50 base learners and the learning rate is kept to 0.1. The final prediction of the ensemble model is a weighted combination of predictions made by each base learner. This algorithm is trained iteratively by adding each new base learner to the ensemble model for improving the performance until it reaches the predefined number of learners, which in this case is 50, as shown in Fig. 4.

The number of learners can be changed according to training requirements. The plot in Fig. 4 shows that MSE improves by increasing the number of learners at cost of increased training time. The generation and training of data are conducted offline and do not contribute to computational time. Once the model is trained, the prediction of bistatic RCS can be accomplished instantly.

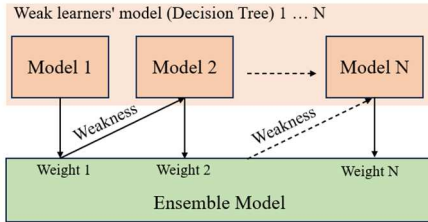


Fig. 3. Ensemble ML model with decision tree base learner

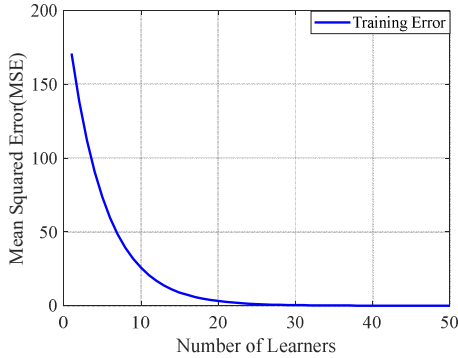


Fig. 4. Training accuracy dependance's on the number of learners

### C. Testing

After training, the model's performance is assessed using unseen testing data, comprising both input  $X_{Test}$  and corresponding output  $Y_{Test}$ . The trained model predicts RCS values based on  $X_{Test}$  inputs, which are then compared with the actual  $Y_{Test}$  RCS values. The MSE is approximately 0.0561 dB, showcasing exceptional accuracy and performance of trained model.

It is important to highlight the limitation of ML approach. Every ML model is trained to work for specific type of input. If there is need to add/remove number of input feature or refining the output, then ML model needs to be trained again. Owing to have a large number of input parameters, the proposed ML approach is not a generalized model that can work for every combination of input parameters.

## IV. SIMULATION ANALYSIS

In this section, two performance parameters are analyzed: accuracy and computational time. To evaluate computational efficiency, two distinct methodologies are employed: RCS prediction time with and without input dataset generation time. Time is measured using MATLAB's 'tic' and 'toc' on the same machine. In the first method, only RCS prediction time for both algorithms are compared utilizing entire input X generated previously for yacht. The input X is given to the ML model and the RCS estimation script of the POfacets tool. Both approaches compute the RCS within seconds utilizing pre-existing dataset however, ML approach outperforms POfacets because of the higher complexity of RCS estimation within the POfacets script. This method is useful when a database of inputs is available, and a quick RCS prediction is needed. In the second method, both input data generation time and RCS prediction are considered. Time taken to generate the 32851 input combinations and their RCS prediction using POfacets is around 16.67 minutes, as shown in Table 1. This time can be further reduced by discretizing azimuth angles with step of  $3^\circ$  instead of  $1^\circ$ , making 11011 combinations. These gaps are then filled by performing interpolation, resulting in 32851 combinations, as those of X. Table 1 shows that generation of dataset with step of  $3^\circ$ , performing interpolation and computing RCS, takes 5.1 minutes, 3.27 times less the time needed by POfacets. This proves that with or without data generation the ML model still outperforms POfacets. The time can be further reduced by increasing step size however, on account of reduced accuracy. This method is useful when there is change in input features like target material, angles and operating frequency, making necessary the generation of a new input dataset to predict the RCS.

Table 1. Computational complexity comparison

Prediction Time with Pre-Existing DataSet		
Methods	Yacht	Tank
Pofacets	3.2415 Seconds	2.8154 Seconds
ML Model	0.2512 Seconds	0.2836 Seconds
DataSet Generation + Prediction Time		
Methods	Yacht	Tank
Pofacets	16.67 Minutes	5.93 Minutes
ML Model	5.1 Minutes	1.8047 Minutes

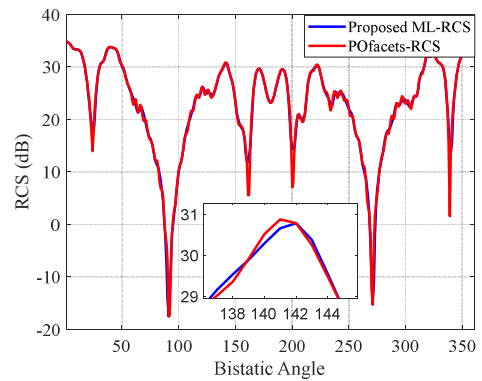


Fig. 5. Bistatic RCS for a Yacht

To evaluate the accuracy, the RCS is estimated using both approaches: POfacets receives the entire input X, while the ML model is provided with the same input with step of  $3^\circ$ . Fig. 5 shows the RCS against bistatic angle  $\phi_{ob} = 0^\circ \div 360^\circ$  at  $\theta_{ob} = 30^\circ$ . It is not feasible to show plots for all angles  $\theta_{ob} = 0^\circ \div 90^\circ$ . Although there is  $3^\circ$  step in the dataset of

ML approach, its accuracy still approaches close to POfacets and follows the same trend with MSE 1.8096 dB. If step size is further increased to  $5^\circ$  to reduce the time, the MSE increases to 3.7738 dB. There is a trade-off between time and accuracy. Finally, two dips in RCS value appear at  $90^\circ$  and  $270^\circ$ , due to orientation of viewpoint of target.

It is important to clarify that there is no need to train the model again for any change in input features like frequency, target, angles unless when adding or subtracting the number of features. The scattered field which is input to ML model contains all the information about target and all operating requirements. Therefore, if any changes are required in inputs like frequency, target type, incident angles, then only the generation of the dataset is required to predict the target RCS. To verify this, let us consider a tank instead of a yacht and a frequency of 3GHz (i.e., S band).

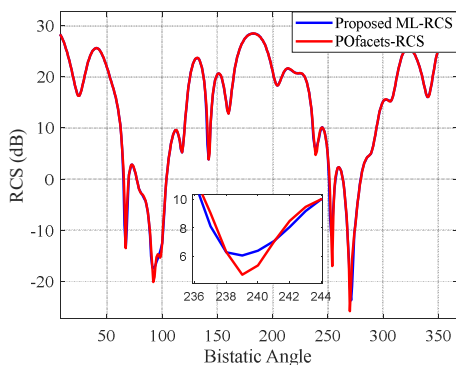


Fig. 6. Bistatic RCS for a Tank

Upon prediction with an already trained model, Fig 6 shows that the proposed algorithm follows the same trend of RCS against bistatic angles as POfacets with MSE of 2.1342 dB. The computational time in Table 1 shows the dominance of ML approach over POfacets. Moreover, this ML model, originally trained on the yacht dataset, has demonstrated outstanding performance also for the tank model.

## V. CONCLUSION AND FUTURE DIRECTION

This paper has introduced an innovative RCS estimation technique for extended targets, leveraging on ensemble ML methods. The proposed approach has been thoroughly examined in a bistatic radar scenario, aiming to improve accuracy and time efficiency in RCS estimation. The simulation results prove that the ML approach is 3.27 times faster than POfacet for yacht RCS estimation, with MSE of 1.8096 dB. This problem may particularly exacerbate in dynamic close-to-reality scenarios, where it is necessary to simulate multiple targets undergoing continuous changes in position and orientation with respect to different RHs.

The model has undergone testing on diverse targets to predict bistatic RCS across a range of bistatic angles, demonstrating outstanding accuracy and computational efficiency. Future enhancement of this ML-based RCS estimation is to compute RCS of each facet making it an efficient RCS predictor for extended targets laying in more than one radar resolution cell.

## VI. ACKNOWLEDGMENT

This work is funded by CLARIFIER (SPS funding scheme by NATO) and by the EU under the Italian National Recovery and Resilience Plan (NRRP) of NextGenerationEU, partnership on “Telecommunications of the Future” (PE00000001 - program “RESTART”).

## REFERENCES

- [1] M. I. Skolnik, Ed., *Radar Handbook*, 3rd Edition. McGraw-Hill Education, 2008. Accessed: Nov. 15, 2023. [Online]. Available: <https://www.accessengineeringlibrary.com/content/book/9780071485470>
- [2] E. Fishler, A. Haimovich, R. Blum, D. Chizhik, L. Cimini, and R. Valenzuela, “MIMO radar: an idea whose time has come,” in *Proceedings of the 2004 IEEE Radar Conference (IEEE Cat. No. 04CH37509)*, Apr. 2004, pp. 71–78. doi: 10.1109/NRC.2004.1316398.
- [3] J. Li and P. Stoica, “MIMO Radar with Colocated Antennas,” *IEEE Signal Process. Mag.*, vol. 24, no. 5, pp. 106–114, Sep. 2007, doi: 10.1109/MSP.2007.904812.
- [4] A. M. Haimovich, R. S. Blum, and L. J. Cimini, “MIMO radar with widely separated antennas,” *IEEE Signal Process. Mag.*, vol. 25, no. 1, pp. 116–129, Jan. 2008, doi: 10.1109/MSP.2008.4408448.
- [5] F. Scotti, S. Maresca, L. Lembo, G. Serafino, A. Bogoni, and P. Ghelfi, “Widely Distributed Photonics-Based Dual-Band MIMO Radar for Harbour Surveillance,” *IEEE Photonics Technol. Lett.*, vol. 32, no. 17, pp. 1081–1084, Sep. 2020, doi: 10.1109/LPT.2020.3012731.
- [6] M. M. H. Amir et al., “Target RCS Modeling and CFAR Detection Performance with Photonics-based Distributed Multi-Band MIMO Radars,” in *2021 21st International Radar Symposium (IRS)*, Jun. 2021, pp. 1–9. doi: 10.23919/IRS51887.2021.9466202.
- [7] B. R. Mahafza, *Radar Systems Analysis and Design Using MATLAB*, 3rd ed. New York: Chapman and Hall/CRC, 2016. doi: 10.1201/b14904.
- [8] T. I. O. Ahmed and M. Mirghani, “Estimation of Radar Cross Sectional Area of Target using Simulation Algorithm,” *Int. J. Res. Stud. Electr. Electron. Eng.*, vol. 4, no. 2, pp. 20–24, 2018.
- [9] “POfacets4.5 - File Exchange - MATLAB Central.” Accessed: Nov. 15, 2023. [Online]. Available: <https://www.mathworks.com/matlabcentral/fileexchange/50602-pofacets4-5>
- [10] M. M. H. Amir et al., “Performance Evaluation of Photonics-Based Coherent MIMO Radar Systems for Maritime Surveillance,” *Inventions*, vol. 8, no. 4, Art. no. 4, Aug. 2023, doi: 10.3390/inventions8040099.
- [11] “Efficient RCS Prediction of the Conducting Target Based on Physics-Inspired Machine Learning and Experimental Design | IEEE Journals & Magazine | IEEE Xplore.” Accessed: Nov. 15, 2023. [Online]. Available: <https://ieeexplore.ieee.org/document/9212600>
- [12] D. Xiao, L. Guo, W. Liu, and M. Hou, “Improved Gaussian Process Regression Inspired by Physical Optics for the Conducting Target’s RCS Prediction,” *IEEE Antennas Wirel. Propag. Lett.*, vol. 19, no. 12, pp. 2403–2407, Dec. 2020, doi: 10.1109/LAWP.2020.3034169.
- [13] F. Ahmad et al., “Performance Enhancement of mmWave MIMO Systems Using Machine Learning,” *IEEE Access*, vol. 10, pp. 73068–73078, 2022, doi: 10.1109/ACCESS.2022.3190388.
- [14] S. Uddin, I. Haque, H. Lu, M. A. Moni, and E. Gide, “Comparative performance analysis of K-nearest neighbour (KNN) algorithm and its different variants for disease prediction,” *Sci. Rep.*, vol. 12, no. 1, Art. no. 1, Apr. 2022, doi: 10.1038/s41598-022-10358-x.
- [15] J.-C. Huang, et al., “Application and comparison of several machine learning algorithms and their integration models in regression problems,” *Neural Comput. Appl.*, vol. 32, no. 10, pp. 5461–5469, May 2020, doi: 10.1007/s00521-019-04644-5.
- [16] T. G. Dietterich, “Ensemble Methods in Machine Learning,” in *Multiple Classifier Systems*, vol. 1857, in Lecture Notes in Computer Science, vol. 1857., Berlin, Heidelberg: Springer Berlin Heidelberg, 2000, pp. 1–15. doi: 10.1007/3-540-45014-9\_1.
- [17] O. Sagi and L. Rokach, “Ensemble learning: A survey,” *WIREs Data Min. Knowl. Discov.*, vol. 8, no. 4, p. e1249, 2018, doi: 10.1002/widm.1249.